Physics Letters A 473 (2023) 128828

Contents lists available at ScienceDirect

Physics Letters A

journal homepage: www.elsevier.com/locate/pla

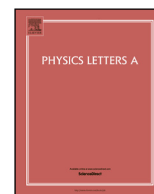

A new absorption-based method of X-ray microscopy using a nanofocusing refractive lens

Victor G. Kohn [a,*], Tatiana S. Argunova [b]

[a] National research centre "Kurchatov Institute", 123182, Moscow, Russia
[b] Ioffe Institute RAS, 194021 St. Petersburg, Russia

ARTICLE INFO

Article history:
Received 22 February 2023
Received in revised form 31 March 2023
Accepted 3 April 2023
Available online xxxx
Communicated by S. Khonina

Keywords:
Synchrotron radiation
Micro-objects
Nanofocusing
Tomography
Micropores
Computer simulations

ABSTRACT

A new method for studying the internal structure of micro-objects using synchrotron radiation based on the use of a planar nanofocusing compound refractive lens is proposed. The method registers the integral intensity of radiation after passing through the object. In this case, locality is ensured by focusing the beam into a line of nanometer width. Phase contrast is not used. The profile of object thickness inside the x-ray beam is obtained immediately. However, the two-dimensional structure of the object image is calculated using the specific tomography method. The method does not require complex mathematical calculations and gives a result with a very high accuracy. An experiment was simulated with a silicon carbide substrate for typical values of all parameters to illustrate the operation of the method.

© 2023 Elsevier B.V. All rights reserved.

1. Introduction

Development of modern industrial technologies for obtaining bulk crystals of silicon carbide (SiC) and sapphire (Al_2O_3) has led to an improvement in their structural homogeneity. However, substrates, made of these crystals and used in electronics, contain pores (for example, in SiC crystals) or gas inclusions (for example, in Al_2O_3 crystals). These pores have become smaller and can be submicron or even nanometer in size. At the same time, the properties of nanoheterostructures grown by epitaxy, as well as graphene, obtained as a result of thermal destruction of the SiC surface [1] or deposition on sapphire [2], depend on the perfection of the substrates. Therefore, increased requirements are placed on diagnostic methods. X-ray techniques play an important role in bridging the gap between optical and electron microscopy.

Synchrotron radiation (SR) makes it possible to study the internal structure of objects and reveal micron-sized pores. However, a simple inline scheme of the experiment, based on taking into account absorption when rays pass through an object, is not applicable to micro-objects [3]. The reason is that, along with absorption, a phase contrast arises. The latter is a local change in the radiation intensity, mainly associated with the interference of rays deflected by the object and passing by it [4–6]. This change in intensity is zero on average. Therefore it does not change the integral intensity. For large object sizes, even in coherent radiation, the phase contrast is averaged, because the oscillation period is very small, and a very high resolution of the detector is not required.

When the size of the object is reduced, either a strong magnification of the image, i.e. X-ray microscopy (XM) [7], or a very high resolution of the position sensitive detector [8] is required. Accordingly, the role of absorption decreases, and the phase contrast has a relatively long period and is easily observed. To observe the phase contrast, high coherence is not required, but it is required for an adequate solution of the inverse problem [9–11]. The reason is that the phase contrast does not directly show the image of the object. This image is presented in the case of absorption by the function $t(x, y)$ of the object thickness along the beam direction (z axis) at the point (x, y) in the plane normal to the beam direction. One has to use special methods for calculating $t(x, y)$ from the local distribution of intensity $I(x, y)$ measured by the position sensitive detector. In the presence of both absorption and phase contrast, the inverse problem is solved poorly and not unambiguously.

Usually, when solving the inverse problem, absorption is neglected, since the changes in intensity with phase contrast are greater than the changes due to absorption. In addition, this approach requires strict control of the degree of coherence. This applies to all methods, including both XM [7] and coherent diffrac-

* Corresponding author.
E-mail addresses: kohnvict@yandex.ru (V.G. Kohn), argunova@mail.ioffe.ru (T.S. Argunova).

https://doi.org/10.1016/j.physleta.2023.128828
0375-9601/© 2023 Elsevier B.V. All rights reserved.

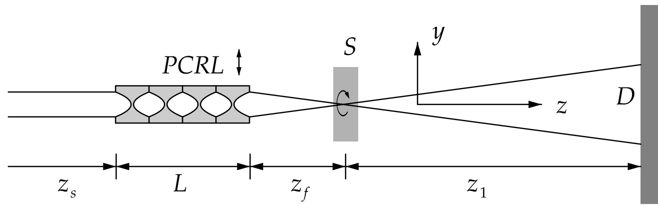

Fig. 1. Scheme of the experiment. z_s is the distance from the source to the PCRL, L is the length of the PCRL, z_f is the focal length, z_1 is the distance from the sample to the detector, $PCRL$ is the planar compound refractive lens, S is the sample, and D is the detector.

tion imaging [12,13] as well as ptychography [14]. Controlling the degree of coherence is a difficult task, as coherence can be destroyed by many factors, not only by the physical size of the source. We also note that a necessary tool for such studies is a position sensitive detector with a high resolution, usually about 1 µm, which is not available to everyone.

In this article we propose a fundamentally different method for imaging micro-objects, which is based only on absorption. It allows one to get an image of an object, that is, a function $t(x, y)$ without solving the inverse phase contrast problem and with any degree of partial coherence. The phase contrast can be eliminated by measuring the integral SR intensity using a detector that sums up all the photons that have passed into the detector. In this case, the phase contrast is averaged and the intensity changes are determined only by absorption.

The locality of information on the object is formed by focusing the beam into a nanometer transverse size using a planar compound refractive lens (PCRL) [15–17]. At present, the technologies for the production of PCRLs have become more complex, and the quality of the PCRLs themselves has greatly increased. We note that the current nanofocusing PCRLs are capable of focusing a beam to a size of no more than 20 nm [18]. Online programs have also been developed that calculate all the beam parameters when focusing with such PCRLs [19].

2. Description of the method of imaging micro-objects

The scheme of the experiment for using the new method is shown in Fig. 1. The SR beam after the monochromator, which is not shown in the figure, is focused by the PCRL in the vertical direction. Usually the vertical dimension of the SR source is smaller than the horizontal one. Accordingly, a smaller transverse beam size can be obtained. A sample, for example, a SiC crystal containing pores of micron size and various shapes, is placed at a focal length z_f from the PCRL, counting from its end. The detector is installed at an arbitrary distance z_1 and measures all the radiation that enters it. The PCRL focuses the beam only in the direction of the Y axis. There is no locality along the X axis and the beam size is limited only by a slit.

PCRL is capable of forming a linear narrow beam with a length of up to 70 µm. The slit can be used to limit the SR beam to smaller values. In this way one point of dependence $I(y)$ is obtained. All points are obtained by moving the PCRL in the vertical direction with a small step. The step of such movement is determined only by the required accuracy of the image. Currently, there are piezo movers capable of moving the sample with a very low speed, which, per step, can reach values of several nanometers. The method described above makes it possible to obtain the dependence on the y-coordinate for the intensity integrated over the x-coordinate. Unfortunately, 2D compound refractive lenses for focusing the beam into a circle of nanometer diameter do not currently exist, and it is not yet clear how these can be performed, in principle.

However, the problem of obtaining two-dimensional dependence in the (x, y) plane can be solved by a special tomography method. If one rotates the sample around the Z axis, two-dimensional data set $I(y, \varphi)$ can be registered, that is a sinogram. It is necessary to rotate the object within the 180 degrees range of φ angle values with a constant step. Then, using the tomography program, the sinogram can be converted into a tomogram which shows the dependence $I(x, y)$. The desired dependence $t(x, y)$ is obtained by taking the logarithm and multiplying by a constant coefficient.

There are no ambiguous mathematical calculations in this method. The resolution of the method is determined by the size of the beam at the focus of the lens. To obtain a small size of the SR beam at the focus, SR coherence is still necessary, since focusing is a special case of the phase contrast. The size of the beam at the focus is determined not only by the PCRL, but also by the transverse size of the SR source. However, coherence may be partial. This simply reduces the resolution, but does not lead to significant errors.

The difference between the new method and the standard tomography method (STM), based on absorption, is that here it is necessary to take the logarithm not of the sinogram, but of the tomogram. At each point we obtain the integral intensity along the transverse coordinate x. In the STM one uses the local intensity along the x coordinate and immediately gets the function $t(x, \varphi)$, where φ is the angle of rotation of the sample around the Y axis while the thickness t itself is the integral over z of the electron density ρ of the material. The result of STM calculations is the function $\rho(x, z)$. In the new method of this article, tomography allows one to get the function $I(x, y)$, which, after taking the logarithm, gives the dependence $t(x, y)$.

It is known that the STM allows one to obtain a 3D dependence $\rho(x, y, z)$. The new method allows one to obtain only one 2D projection $t(x, y)$. It is only 2D image of the object, namely, an integral of $\rho(x, y, z)$ over z coordinate. The function $t(x, y)$ is obtained in the STM directly by a position sensitive detector for one measurement. However, the STM is not applicable for micro-objects due to existence of the phase contrast.

The special tomography method has a peculiarity that is described below. If one uses the filtered back projection (FBP) algorithm [20], it is necessary to calculate the Fourier transform within the finite region. It is assumed in these calculations that the function is equal to zero outside this region, and the same should be on its boundaries. But the function $I(x, y)$ cannot be equal to zero. If it is normalized to unity outside the object, therefore it is equal to unity on the boundaries. It looks as a jump exists at the border of the region, which leads to a strong artifact. As a result, the calculation shows the background which is close to zero only in the center of the region, and it increases very strongly near the boundaries. The described situation can be corrected as follows. When normalizing the intensity outside the object by unity, it is necessary to subtract the unity at each point of the object when calculating the sinogram, that is, to subtract the number of points of the computational grid from each sinogram value. After the calculation it is necessary to add this unity to each point of the tomogram.

Since in this method the contrast is determined only by absorption, it will be weak for micro-objects, and it is better to use radiation with low photon energy. On the other hand, it is necessary to have many photons to prevent spoiling the contrast by shot noise, because it is known that the relative magnitude of shot noise is equal to one divided by the square root of the number of photons. Therefore, when studying pores in crystals, one should try to have samples as thin as possible.

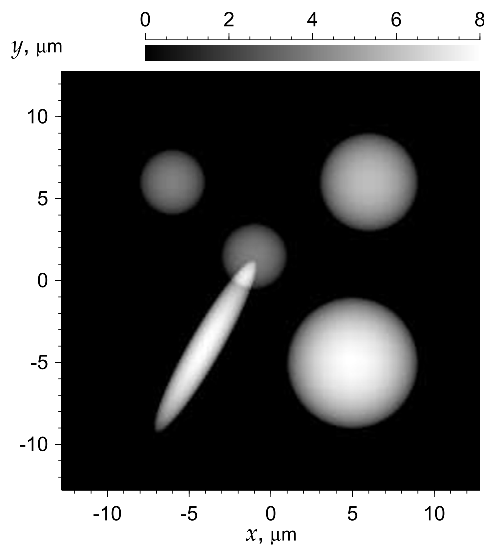

Fig. 2. Function $t(x, y)$ of the initial thickness of voids along the direction of beam propagation for the modeled sample in the transverse plane on the computational grid with a linear size of 25.6 µm. The sample has 4 spherical pores and one ellipsoid, which partially overlaps with the spherical pore. The diameter of the largest spherical pore is 8 µm.

3. Computer simulation of the experiment

As an illustration of the method, we performed a computer simulation of the experiment for the following parameters: photon energy 6.2 keV, vertical size of the source 100 µm, distance from the source to the PCRL $z_s = 14$ m. The parameters of the SR source correspond to the 2nd generation source at the Kurchatov Institute (Moscow) [21]. The PCRL on the silicon surface has 10 elements with an aperture of 50 µm, a radius of curvature of 6.25 µm, and a material thickness between the parabolic surfaces of 2 µm. The calculation using the online program [19] for the specified conditions gives a full width at half maximum (FWHM) of 0.332 µm for the Gaussian curve of SR intensity at the focus, while for a point source the FWHM is 0.282 µm, i.e., the source size increases the beam FWHM at the focus by only 18%.

The sample is a silicon carbide (SiC) crystal plate with pores of various shapes and sizes. Fig. 2 shows the $t(x, y)$ function for a simulated sample with pores. The function shows the pore thickness along the direction of the SR beam in the transverse plane. If there are no pores $t = 0$ (black color). This is the minimum pore thickness. The maximum is $t_m = 8$ µm (white color). The linear size of the computational domain is 25.6 µm. For calculations, a grid of points with a step of 0.1 µm and a number of points of 256 was used. The grid spacing corresponds to the vertical scanning spacing of the focused beam through the sample. The picture shows 4 spheres with diameters of 4, 6 and 8 µm and an ellipsoid with diameters of 2, 12 and 8 µm along the X, Y and Z axes, respectively. The ellipsoid is rotated 30 degree from the vertical axis.

These data were used to calculate the sinogram shown in Fig. 3. Here the horizontal dimension is again 25.6 µm, and the vertical dimension corresponds to the range of angles from −90 to 90 degrees, which was calculated in 1 degree increments. The function $t(x, y)$ shown in Fig. 2 was used to calculate the distribution of the difference in the intensity of the beam transmitted through the sample $I(x, y) = \exp(\mu\, t(x, y))$. Here μ is the absorption coefficient of SR in a SiC crystal for the chosen photon energy. In this case, $\mu = 0.02998$ µm^{-1}. The presence of a void in the material leads to increase in intensity, which, in the absence of a void, is normalized to unity.

The function $I(x, y)$ was summed over all points of the X axis for different values of the angle φ of sample rotation around the

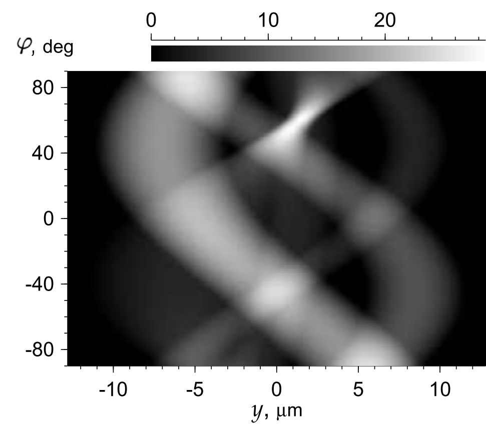

Fig. 3. A sinogram representing simulated experimental data. The horizontal axis is the y coordinate, and the vertical axis is the rotation angle φ of the sample. The function is the difference in the intensity integrated over the x coordinate due to the presence of pores in the sample.

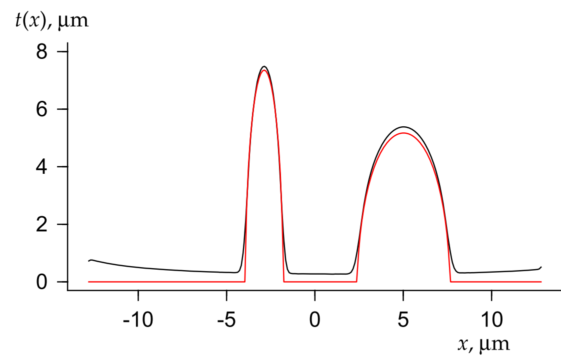

Fig. 4. Detailed comparison of the initial (red curve) and calculated from the tomogram (black curve) function $t(x, y)$ at $y = -2$ µm.

Z axis, which corresponds to the sinogram $I(y, \varphi)$. The size of the beam at the focus was taken into account by calculating the convolution of $I(y)$ and a Gaussian function, which has FWHM of 0.332 µm, as indicated above, at each value of the angle of rotation. In addition, at each point of the y-dependence, the number of points 256 was subtracted to obtain a minimum of zero. As a result, it turned out that the minimum on the sinogram is zero with high accuracy and the maximum is 28.6 µm.

The sinogram simulates experimental data. The calculation of the tomogram was carried out using our own program which implements the FBP algorithm [9]. After the calculation, the unity was added to each point. The calculation result in a form similar to Fig. 1 is not shown because a difference of the calculated function from the original one is so weak that the low resolution of the drawing is unable to show it. Note that the change in intensity $I(x, y)$ obtained as a result of the calculation is in the range from 1.006 to 1.277. That is, the contrast, defined as the ratio of the difference to the sum of the indicated values, is 0.12, which is not so small. Dependence $t(x, y)$ is obtained after taking the logarithm of the tomogram and dividing by μ.

The difference between the calculated distribution and the original one can be estimated from the minimum and maximum values. The values obtained were 0.26 µm and 8.22 µm, respectively. That is, the calculated distribution turned out to be higher than the original distribution, although all object sizes are reproduced with relatively high accuracy. Fig. 4 shows a comparison of the original $t(x)$ curve at a height of $y = -2$ µm with that calculated from the sinogram after taking into account the beam size. One can see that, on the whole, the method describes the objects well, but is not able to describe sharp thickness variation at their boundaries,

as well as the fact of object absence. The background, although not very high, is still not equal to zero. Even narrower beams are needed to improve accuracy. It is also necessary to search for a more advanced sinogram processing algorithm to eliminate the defect of using the finite dimensions of the computational domain.

CRediT authorship contribution statement

Victor G. Kohn: Writing – original draft, Software, Investigation. **Tatiana S. Argunova:** Writing – review & editing, Conceptualization.

Declaration of competing interest

The authors declare that they have no known competing financial interests or personal relationships that could have appeared to influence the work reported in this paper.

Data availability

Data will be made available on request.

Acknowledgements

The work of V.G. Kohn was carried out partly with the financial support of the Ministry of Science and Higher Education of the Russian Federation, project 075-15-2021-1362, and partly at the expense of the RFBR grant 19-29-12043 mk. The work of T.C. Argunova was carried out partly with the financial support of the RFBR grant 19-29-12041 mk, and partly at the expense of the Ministry of Science and Higher Education of the Russian Federation, project 075-15-2021-1349.

References

[1] A.A. Lebedev, S.Yu. Davydov, I.A. Eliseyev, A.D. Roenkov, O. Avdeev, S.P. Lebedev, Y. Makarov, M. Puzyk, S. Klotchenko, A.S. Usikov, Materials 14 (2021) 590.
[2] J. Shan, J. Sun, Z. Liu, Chem. Nanomater. 7 (2021) 515.
[3] P.J. Withers, C. Bouman, S. Carmignato, V. Cnudde, D. Grimaldi, K. Hagen, K. Charlotte, E. Maire, M. Manley, A. Du Plessis, S.R. Stock, Nat. Rev. Methods Primers 1 (2021) 18.
[4] A. Snigirev, I. Snigireva, V. Kohn, S. Kuznetsov, I. Schelokov, Rev. Sci. Instrum. 66 (1995) 5486–5492.
[5] T.S. Argunova, V.G. Kohn, Phys. Usp. 62 (2019) 602–616.
[6] Siwei Tao, Congxiao He, Xiang Hao, Cuifang Kuang, Xu Liu, Appl. Sci. 11 (2021) 2971.
[7] A. Bosak, I. Snigireva, K.S. Napolskii, A. Snigirev, Adv. Mater. 22 (2010) 3256–3259.
[8] A. Koch, C. Raven, P. Spanne, A. Snigirev, J. Opt. Soc. Am. A 15 (1998) 1940–1951.
[9] V.G. Kohn, Phys. Scr. 56 (1997) 14–19.
[10] D. Paganin, S.C. Mayo, T.E. Gureyev, P.R. Miller, S.W. Wilkins, J. Microsc. 206 (2002) 33–40.
[11] V.G. Kohn, T.S. Argunova, J.H. Je, J. Phys. D, Appl. Phys. 43 (3) (2010) 442002.
[12] H.N. Chapman, K.A. Nugent, Nat. Photonics 4 (2010) 833–839.
[13] J. Miao, T. Ishikawa, I.K. Robinson, M.M. Murnane, Science 348 (2015) 530–535.
[14] F. Pfeiffer, Nat. Photonics 12 (2018) 9–17.
[15] C.G. Schroer, M. Kuhlmann, U.T. Hunger, T.F. Gunzler, O. Kurapova, S. Feste, F. Frehse, B. Lengeler, M. Drakopoulos, A. Somogyi, A.S. Simionovici, A. Snigirev, I. Snigireva, C. Schug, W.H. Schroder, Appl. Phys. Lett. 82 (2003) 1485–1487.
[16] A. Snigirev, I. Snigireva, V. Kohn, V. Yunkin, S. Kuznetsov, M.V. Grigoriev, T. Roth, G. Vaughan, C. Detlefs, Phys. Rev. Lett. 103 (2009) 064801.
[17] A. Snigirev, I. Snigireva, M. Lyubomirskiy, V. Kohn, V. Yunkin, S. Kuznetsov, Opt. Express 22 (2014) 25842–25852.
[18] V.G. Kohn, M.S. Folomeshkin, J. Synchrotron Radiat. 28 (2021) 419.
[19] V.G. Kohn, http://kohnvict.ucoz.ru/jsp/1-crlpar.htm.
[20] A.C. Kak, M. Slaney, Principles of Computerized Tomographic Imaging, Society for Industrial and Applied Mathematics, 2001, 322 pp.
[21] V.G. Kohn, A.G. Kulikov, P.A. Prosekov, A.Yu. Seregin, A.V. Targonsky, Ya.A. Eliovich, Yu.V. Pisarevsky, A.E. Blagov, M.V. Kovalchuk, J. Synchrotron Radiat. 27 (2020) 378–385.